27th EPS Conference on Contr. Fusion and Plasma Phys. Budapest, 12-16 June 2000 ECA Vol. **24B** *(2000) 548 -551*

H–Mode Edge-Driven Instabilities as Low-n Kink/Ballooning Modes

J.R. Ferron, L.R. Baylor,[1] M.S. Chance,[2] M.S. Chu, G.L. Jackson, L.L. Lao, M. Murakami,[1] T.H. Osborne, P.B. Snyder, E.J. Strait, A.D. Turnbull, and M.R. Wade[1]

General Atomics, P.O. Box 85608, San Diego, California
[1]Oak Ridge National Laboratory, Oak Ridge, Tennessee.
[2]Princeton Plasma Physics Laboratory, Princeton, New Jersey.

ABSTRACT

Comparisons of measured ELM characteristics and edge pressure gradient to a model for H–mode edge region ideal MHD stability are described. The dependence on discharge shape indicates that Type I ELMs in typical DIII–D discharges result from low-n kink/ballooning instabilities triggered at pressure gradient values significantly above the high-n ballooning mode stability threshold.

The H–mode edge region transport barrier results in a large pressure gradient that can drive instabilities. In many cases the edge region collisionality is sufficiently low that a large bootstrap current accompanies the pressure gradient. This current density adds another instability drive. Thus, edge localized modes (ELMs) are a typical characteristic of tokamak discharges operating in H–mode [1]. The relatively large, Type I ELMs that occur when the auxiliary heating power is sufficiently far above the H–mode power threshold have been attributed in various experiments to either high toroidal mode number (n) ballooning modes driven by the pressure gradient or to low n kink modes for which the current density drive is also significant [2].

In a series of experiments in the DIII–D tokamak, the edge region stability boundaries were changed from a regime in which high n ballooning modes were expected to be the most unstable to a regime in which lower n kink/ballooning modes would be expected to dominate. This change in stability boundaries was a result of changes in the discharge shape [3]. The observed changes in the ELM character and the edge region pressure gradient (P'_{edge}) were consistent with changes in n of the most unstable mode. Comparison of the results from these experiments with ideal MHD stability threshold calculations shows that Type I ELMs in typical DIII–D single-null and double-null divertor shapes most likely result from low-n kink/ballooning modes. The experiments and comparison with theory are briefly summarized here. More detailed descriptions can be found in Refs. [4,5].

The dependence of the H–mode edge region stability boundaries on discharge shape is summarized in a schematic, shown in Fig. 1, that was derived from the predictions of ideal MHD theory and the results of the experiments. Although both P' and current density are instability drives, the current density in the edge region is expected to be primarily bootstrap current which depends on P'_{edge}, so the stability threshold is illustrated in the figure as a function of P'_{edge} and n.

Figure 1 illustrates the important role that access to a second regime of stability plays in determining the most unstable mode in the H–mode edge region. In discharges with a shape with sufficiently low or high squareness, represented by the high squareness ($\delta_2 = 0.5$) curve in the figure, there is no edge region access to the second stability regime at any value of n. In this case (operating Point 1 in Fig. 1) the observed value of P'_{edge} is equal, within measurement uncertainties, to the calculated stability threshold for the high-n ballooning mode [5]. The toroidal mode number of edge instabilities is expected to be approximately 40, because higher mode number instabilities are stabilized by finite Larmor radius. The energy loss

from an ELM is expected to decrease with decreasing P'_{edge} [1,6] and, in addition, higher mode number, shorter wavelength instabilities will perturb a smaller region of the discharge [7], causing a smaller energy loss. Recovery from a small energy loss is quicker resulting in higher ELM frequency. Consistent with these expectations, the ELMs in high squareness discharges without second stability regime access have relatively high frequency, 4 kHz, with the edge T_e perturbation below the measurement limit.

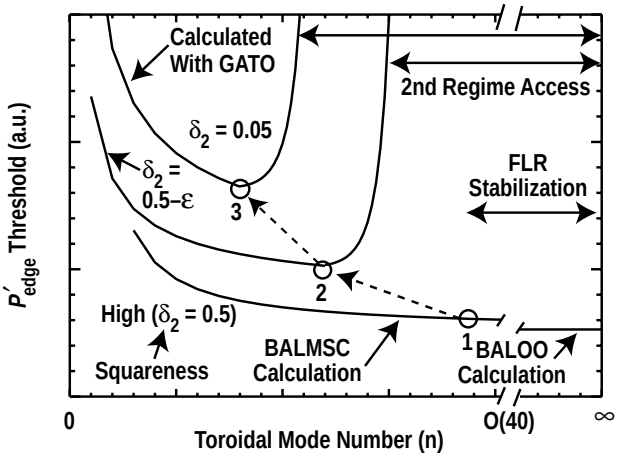

Fig. 1. A schematic drawing of the pressure gradient stability threshold in the H–mode pedestal region for three different discharge shapes. Here, δ_2 is the discharge shape squareness and ε represents a small value.

Discharge shapes with mid-range values of squareness are expected to have access to a second stability regime over a range of values of n, as illustrated by the top two curves in Fig. 1. There is a threshold value of n for second regime access [4] that is expected to vary with discharge shape. For values of n below this threshold the P'_{edge} stability threshold is predicted [4] to increase as n decreases. Thus, for a given discharge shape, the most unstable mode is expected to have n near the second regime access threshold.

These predictions are consistent with observations in the experiment. Factor of 10 decreases in the ELM frequency and corresponding increases in ELM amplitude were observed in the experiment [4,5] to result from the changes in shape, squareness or triangularity [8], represented by each shift in operating point (from 1 to 2 and from 2 to 3) shown in the Fig. 1 schematic. This is consistent with a decrease in n of the most unstable mode as the shape is changed.

In Fig. 2 the measured values of P'_{edge} are summarized as a function of discharge shape squareness and compared to predicted stability thresholds for the ideal infinite-n ballooning and ideal low-n kink/ballooning modes. For this comparison, the stability threshold for low-n modes is represented by the calculated value for n = 5 and the stability threshold for infinite-n modes is represented by the value for a model equilibrium with magnetic shear sufficiently high that there is no second stability regime access. In the figure, the data points at high (δ_2 = 0.5) and low (δ_2 = 0.0) squareness values shown as diamonds represent discharges with high frequency ELMs and no ballooning mode second stability regime access (like operating point 1 in Fig. 1). The measured pressure gradient values for these points agree well with the calculated ballooning mode first stability regime limit. The higher P'_{edge} values plotted at the same squareness (shown as triangles) were measured when a small shift in shape or edge current density resulted in second stability regime access [5].

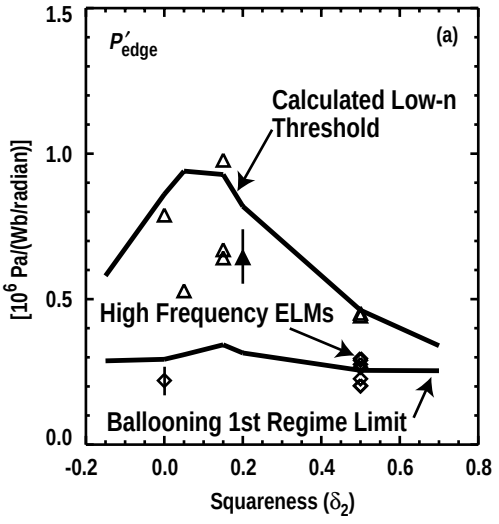

Fig. 2. Measured total P'_{edge} as a function of discharge shape squareness in double-null divertor shapes.

The pressure gradient values measured during low frequency ELMs (triangles, Fig. 2) show scaling with discharge shape that agrees with that of the predicted low-n stability threshold. Both the measured pressure gradient values and the predicted low-n threshold are well above the ballooning mode stability limit and increase significantly as the squareness is reduced from $\delta_2 = 0.5$ to $\delta_2 = 0.15$.

The predicted low-n pressure gradient stability threshold decreases as the width of the H–mode pedestal increases. Stability calculations demonstrating this result are presented in Ref. [4]. An experimental demonstration of this trend is shown in Fig. 3. This figure shows a discharge into which a deuterium pellet was injected early in the ELM-free phase of the H–mode. The result was a rapid increase in the edge pressure gradient resulting in the start of the ELMing phase of the discharge within 50 ms. In this case the pressure gradient just prior to an ELM increased with time after the first ELM. The 7th ELM was triggered at a pressure gradient almost twice that prior to the first ELM. This increase in the ELM pressure gradient threshold occurred while a transient increase in the pedestal width generated by the pellet decayed away, consistent with the predicted pedestal width dependence of the threshold. The changes in both the peak pressure gradient prior to an ELM and the width of the pressure gradient peak are illustrated by the pressure gradient profiles in Fig. 3(b).

When magnetic precursors to Type I ELMs are measured, their characteristics are consistent with low-n instabilities, but this type of indication of mode number from direct experimental measurements is relatively rare. A possible explanation for this is that the toroidal and poloidal mode numbers are sufficiently high that the precursor amplitude at the magnetic probe location outside the plasma is too low to measure. A second possibility is that the instability grows as a locked mode so that a precursor fluctuation is not visible. Precursors to Type I ELMs have been measured in DIII–D in two cases. Particularly in VH–mode discharges, the first one or two ELMs can be exceptionally large and often just prior to these initial ELMs a rotating magnetic perturbation with n in the range 2–9 can be observed [3,9]. One of the few situations in which a precursor oscillation is observed in DIII–D during continuous Type I ELMs is in recent experiments with the neutral beam injection direction opposite to that of the plasma current (counter-injection) [10]. An example is shown in Fig. 4 which indicates n = 6. (Similar observations have been made in ASDEX-U counter-injection discharges [11]). The perturbation growth time is short, approximately 50 μs, indicating an ideal mode.

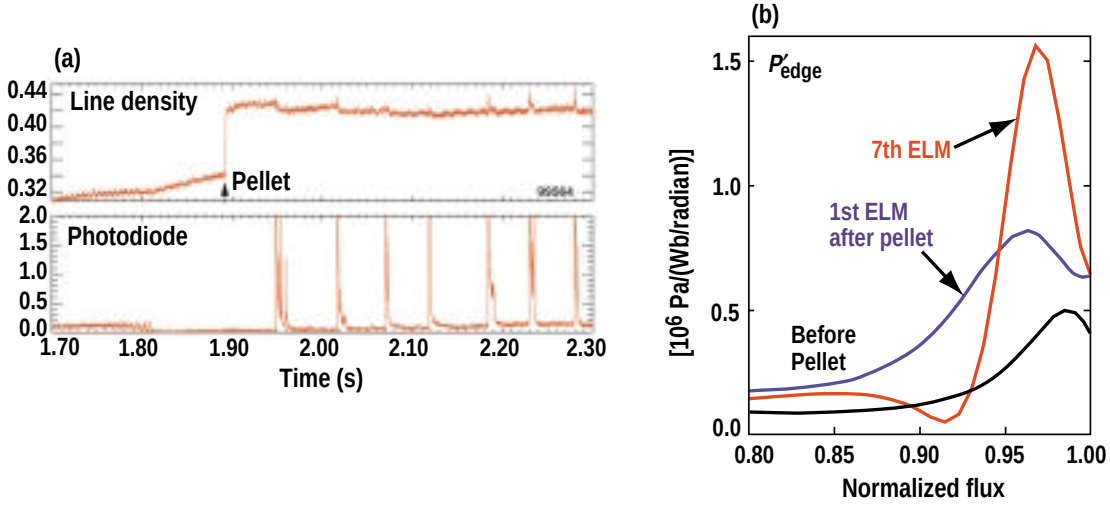

Fig. 3. (a) Time history of parameters for a discharge into which a deuterium pellet was injected early in the ELM-free phase. (b) Profiles of the pressure gradient in the edge region of the discharge just prior to the pellet injection and the first and seventh ELMs.

In conclusion, in both the experiment and theory there are distinct differences between conditions where the pressure gradient is limited by the high-n ballooning mode and conditions where it is limited by low mode number coupled kink/ballooning modes. The experiments with variation in discharge shape squareness show strong evidence of a transition across a stability boundary that controls second stable regime access [5]. In discharges where ballooning mode second stable regime access is expected, the measured pressure gradient values and the calculated pressure gradient thresholds are well above the predicted ballooning first stability regime limit. The observed and calculated strong scaling of the pressure gradient threshold with discharge shape, squareness and triangularity [4], are in good agreement for low-n kink/ballooning instabilities while the infinite-n ballooning mode first regime limit shows little variation with shape (Fig. 2). Finally, the dependence of the pressure gradient threshold on the pedestal width (Fig. 3) indicates an instability that averages the full pressure gradient profile, a low n mode, rather than a high n ballooning mode that depends primarily on the local parameters near a flux surface. Typical DIII–D single-null and double-null discharges have shapes in which a second stability regime is readily accessible in the H–mode edge region. This leads to the conclusion that typical DIII–D H–mode discharges with continuous Type I ELMs are best represented by operating Point 3 shown in the Fig. 1 schematic where the most unstable mode is in the kink/ballooning range of n. Ongoing work to strengthen these conclusions is focusing on stability calculations to show access to the second stability regime at relatively low values of n [12] and improved measurement of the current density profile in the H–mode edge region.

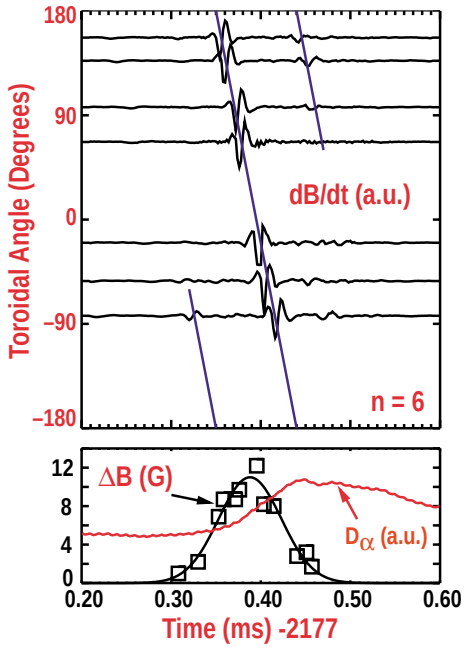

Fig. 4. (a) Magnetic field perturbations measured at various toroidal angles just prior to and during an ELM showing a rotating n = 6 ELM precursor. The value of n was computed from the width of the perturbation and the propagation velocity. (b) Time histories of the amplitude of the magnetic perturbation and the D_α signal during the ELM.

This is a report of work supported by the U.S. Department of Energy under Contract Nos. DE-AC03-99ER54463, DE-AC05-00OR22725, and DE-AC02-76CH03073.

[1] Connor, J.W., Plasma Phys. Contr. Fusion **40**, 531 (1998).
[2] Strait, E.J., et al., in Proc. of the 20th EPS Conf. on Contr. Fusion and Plasma Phys., Lisbon, Portugal, 1993 (European Physical Society, 1993) Vol. 17C, Part I, p. 211.
[3] Miller, R.L., et al., Plasma Phys. Contr. Fusion **40**, 753 (1998).
[4] Ferron, J.R., et al., Phys. Plasmas **7**,1976 (2000).
[5] Ferron, J.R., et al., "Modification of tokamak edge instability character through control of ballooning mode second stability regime accessibility," to be published in Nucl. Fusion (2000).
[6] Connor, J.W., Plasma Phys. Contr. Fusion **40**, 191 (1998).
[7] Connor, J.W., R.J. Hastie, H.R. Wilson, R.L. Miller, Phys. Plasmas **5**, 2687 (1998).
[8] Osborne, T.H., et al., "The effect of plasma shape on H-mode pedestal characteristics on DIII-D," Plasma Phys. Contr. Fusion (to be published).l
[9] Lao, L.L., et al., Nucl. Fusion **39**, 1785 (1999).
[10] Burrell, K.H., et al., Bull. Am. Phys. Soc. **44**, 127 (1999).
[11] Kass. T., S. Gunter, M. Maraschek, W. Suttrop, H. Zohm, Nucl. Fusion **38**, 111 (1998).
[12] Snyder, P., et al., this conference.